

Heteroatom-Stabilized Chiral Framework of Aluminophosphate Molecular Sieves**

Xiaowei Song, Yi Li, Lin Gan, Zhuopeng Wang, Jihong Yu,* and Ruren Xu

Chiral zeolitic materials, which can combine both shape- and enantioselectivity, are important because of the increasing demand for materials used in enantioselective catalysis and separation.^[1] Although chirality is commonly observed in nature and life systems, its occurrence in zeolite materials is particularly rare. The synthesis of such materials remains a significant challenge in the field of zeolite science. To date, among the four-connected zeolite structure types reported, only a few exhibit chiral frameworks.^[2–5] A notable example is aluminosilicate zeolite beta, which has one chiral polymorph (A).^[2] Recently, Zou and co-workers reported a chiral silicogermanate zeolite framework with helical 10-ring channels.^[6] Although the occurrence of chiral zeolite structures is rare, the number of theoretically feasible chiral zeolite frameworks is, in fact, enormous. We have developed a method for the design of chiral zeolite frameworks with specified pore geometries through the constrained assembly of atoms.^[7] According to the calculation results, most four-connected frameworks generated with chiral channels are energetically unfavorable for the SiO₂ composition because of the special geometric strains in such structures. This result suggests that introducing other elements, such as Be, B, Ge, As, or transition metals, instead of Si, might be a promising strategy for stabilizing such frameworks, as they could offer a more reasonable bonding geometry, in terms of bond distances and angles, than a SiO₂ composition does.^[8]

Aluminophosphate molecular sieves, denoted as AlPO₄-*n*, constitute an important family of zeolite materials.^[9,10] The incorporation of transitional-metal ions into the framework sites of AlPO₄-*n* molecular sieves to yield MAPO materials (M = metal ion) is of particular interest for the design of novel single-site solid catalysts in the general quest for clean technology and green chemistry.^[11,12] In contrast to their aluminosilicate zeolitic analogues, aluminophosphate molecular sieves have the advantage of enabling a variety of

metallic ions to substitute isomorphously at tetrahedral sites to form single-site solid catalysts. In these single-site solid catalysts, the active centers at a solid surface are spatially well separated so that an incoming species experiences the same energetic interaction between it and each one of the active centers.^[13] Such materials open up a wide range of catalytic processes for selective oxidations that can be carried out by employing single-site solid catalysts in oxygen or air. Single-site chiral catalysts produced by immobilization of chiral active centers in the nanopores of mesoporous materials have been explored for asymmetric catalysis.^[14] However, single-site solid catalysts with intrinsic chirality have been rarely explored. Recently, theoretical work by Gómez-Hortigüela et al. demonstrated the effect of fluorine-containing chiral templates on the distribution of Mg cations in the structure of MgAPO-5, which is important for potential asymmetric catalysis.^[15] Chiral heteroatom-containing aluminophosphate molecular sieves will be highly desirable for enantioselective conversions by taking advantage of chiral single-site solid catalysts. In this work, we have for the first time synthesized novel heteroatom-containing chiral aluminophosphate molecular sieves (C₄H₁₂N)₂[M₂Al₁₀P₁₂O₄₈] (denoted MAPO-CJ40, M = Co, Zn), with one-dimensional helical 10-ring channels. The framework is intrinsically chiral and exhibits a new zeotype structure. Notably, a helical arrangement of Co cations is observed along the channel. The substitution of Co²⁺ for Al³⁺ in the chiral framework has been further studied by molecular mechanics simulations. Significantly, the circular dichroism (CD) spectrum of CoAPO-CJ40 in a KBr pellet exhibits a strong positive Cotton effect, indicating that the resultant crystals have optical activity.

MAPO-CJ40 samples (M = Co, Zn) were prepared by the solvothermal reaction of a mixture of Co(NO₃)₂·6H₂O (or Zn(NO₃)₂·9H₂O), Al(OiPr)₃, diethylamine, H₃PO₄, tetraethylene glycol, and H₂O in a molar ratio of 0.19:1:6.81:8.22:11.19:26.76 at 180 °C for 12 days in a teflon-lined stainless-steel autoclave. Their phase purity was confirmed by the correlation between the experimental X-ray diffraction (XRD) pattern and the simulated pattern based on structure analysis (Supporting Information Figure S1).

MAPO-CJ40 molecular sieves (M = Co, Zn) crystallize in the orthorhombic space group *P*₂₁₂₁ (No. 19). Their structures are based on the strict alternation of MO₄ (M = Al, Co, Zn) and PO₄ tetrahedra to form an anionic [M₂Al₁₀(PO₄)₁₂]^{2–} framework. Charge neutrality is achieved by extra-framework protonated diethylamine cations. The tetrahedra occupy six independent crystallographic positions: three of these sites are occupied by P atoms, two of them by Al atoms, and the remaining one is shared equally by Co or Zn and Al atoms (Supporting Information Figure S2). The P–O and Al–

[*] X. Song, Dr. Y. Li, L. Gan, Z. Wang, Prof. J. Yu, Prof. R. Xu
State Key Laboratory of Inorganic Synthesis and Preparative
Chemistry, College of Chemistry, Jilin University
Changchun 130012 (China)
Fax: (+86) 431-8516-8608
E-mail: jihong@jlu.edu.cn

[**] This project is supported by the National Natural Science
Foundation of China and the State Basic Research Project of China
(grants 2006CB806103 and 2007CB936402). We thank Prof. Michael
O’Keeffe and Dr. Charlotte Bonneau for their help and valuable
discussions, Prof. Jinglin Zuo for his assistance with the circular
dichroism (CD) analysis, and Dr. Lynne McCusker for her advice on
structure characterization.

Supporting information for this article is available on the WWW
under <http://dx.doi.org/10.1002/anie.200803578>.

O bond lengths ($\text{P}-\text{O}_{\text{av}}$ 1.516; $\text{Al}-\text{O}_{\text{av}}$ 1.726 Å) are in good agreement with those observed in other aluminophosphate molecular sieves. The $\text{Al}(\text{M})-\text{O}$ bond lengths ($\text{Al}(\text{Co})-\text{O}_{\text{av}}$ 1.806(5); $\text{Al}(\text{Zn})-\text{O}_{\text{av}}$ 1.807(0) Å) lie between the range of typical $\text{Al}-\text{O}$ (1.73 Å) and $\text{M}-\text{O}$ bond lengths ($\text{Co}-\text{O}$ 1.96; $\text{Zn}-\text{O}$ 1.956 Å), which is reasonable for cobalt and zinc aluminophosphates.^[16]

The framework of MAPO-CJ40 possesses one-dimensional helical channels running along the [010] direction. Figure 1 a,b shows the framework structure of CoAPO-CJ40. The channels have a 10-ring opening with the pore size of 4.41×2.24 Å ($\text{O}\cdots\text{O}$ distances). Strikingly, the Co atoms adopt a helical arrangement along the channel (Figure 1 b). The helical channels are enclosed by double helical ribbons of the same handedness made of the edge-sharing of six-rings along the 2_1 screw axis (Figure 1 c).

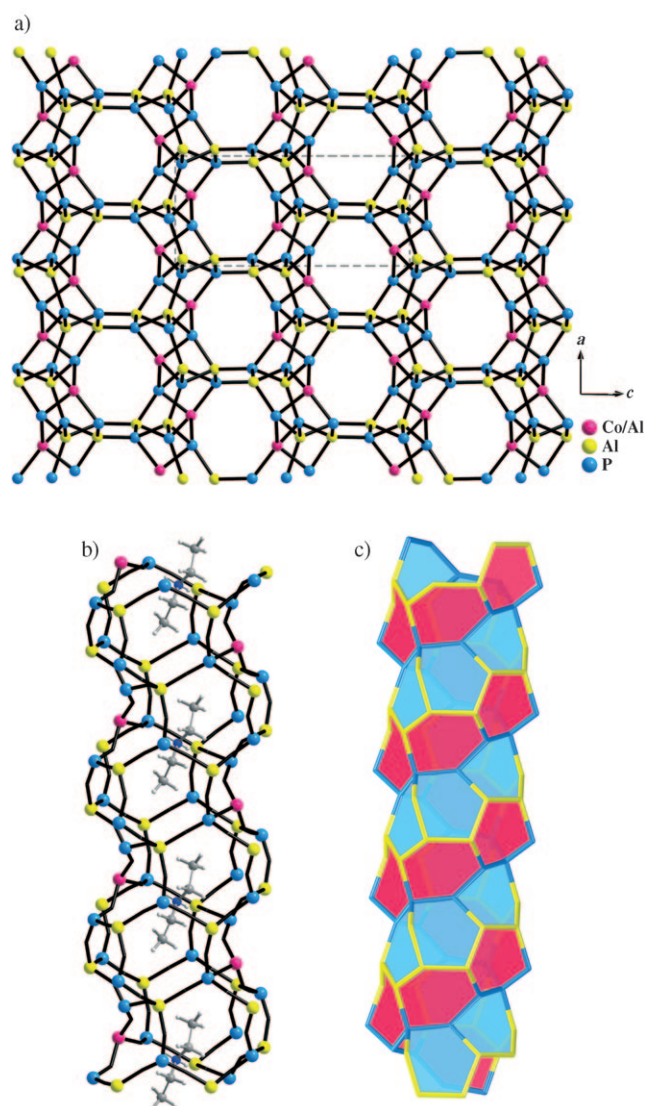


Figure 1. Framework structure of CoAPO-CJ40: a) viewed along the [010] direction. b) The helical 10-ring channel and helical arrangement of cobalt atoms (shown in pink). c) The 10-ring channel enclosed by double-helical ribbons made of the edge-sharing of 6-rings.

Figure 2 a shows the framework of CoAPO-CJ40 viewed along the [100] direction. It can be clearly seen that the whole framework is constructed from the characteristic columns

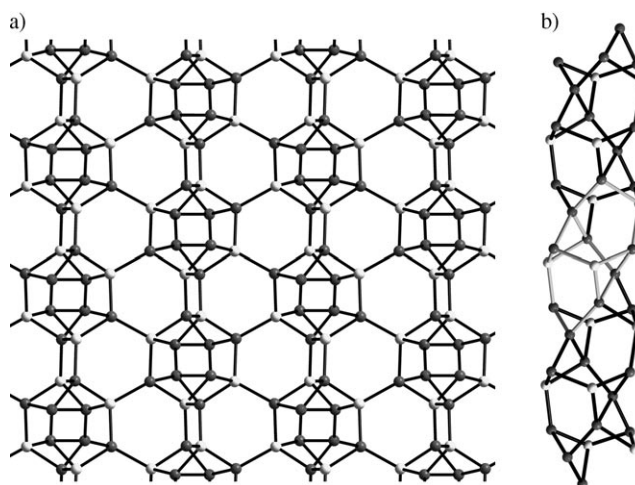


Figure 2. a) Framework structure of CoAPO-CJ40 viewed along the [100] direction. Dark spheres P and Al, light spheres Co/Al. b) The *bog* column. One of the *bog* compositional building units is highlighted (light-colored bonds).

connected through bridging oxygen atoms. These columns are formed by the *bog* compositional building units^[17] sharing the common six-rings (Figure 2 b). Such *bog* compositional building units have been found in some zeolites, such as AEL, AET, AFI, AFO, AHT, ATV, and BOG.^[17] In these frameworks, the *bog* compositional building units are connected in a linear fashion through the sharing of the common edges or four-rings, which is different from the arrangement of the *bog* building units in CoAPO-CJ40. It should be noted that each *bog* column consists of two types of concentric helical chains with the same handedness running along the [100] direction. These helical features give rise to the chirality of the framework.

The protonated diethylamine cations reside in the helical channels in a disordered fashion. Hydrogen bonds exist between the N atoms of the diethylamine molecules and the bridging O atoms of the framework. Each diethylamine molecule interacts with the inorganic framework through two hydrogen bonds with $\text{N}\cdots\text{O}$ separations of 2.91(4) and 2.93(4) Å. The framework of MAPO-CJ40 collapses after the removal of the occluded template molecules upon calcination at 600 °C.

At present, 179 zeolite framework types have been reported.^[17] MAPO-CJ40 exhibits a new zeolite framework. It has a framework density of 18.1 T/1000 Å³, which is comparable to zeolites with 10-ring channels. The framework of MAPO-CJ40 can also be described as a three-periodic net with higher symmetry. The intrinsic symmetry of this underlying net, as determined by Systre,^[18] is $I2_12_12_1$ with three different T sites. This means that the framework of MAPO-CJ40 is intrinsically chiral. In contrast, some chiral open-framework structures, such as UCSB-7, are not intrinsically chiral.^[5] The chirality of those structures may come from the

arrangement of different element species, but not from their underlying nets. The vertex symbols for the three T sites in the net of MAPO-CJ40 are 4.6.4.6₄.6.6₃, 4.6₃.6.6₂.6.6₂, and 4.6.6.6₃.6.6₃.10₉. This three-periodic net is carried by a unique natural tiling with the transitivity of (3 9 10 6) (Supporting Information Figure S3).^[19] There are six different tiles in this tiling, with the face symbols [4.6²], [6³], [4².6²], [6².10²], and two with [6.10²]. The signature of this tiling is 2[4.6²] + 2[6³] + 4[6.10²] + [4².6²] + [6².10²]. One of the most important advantages of the tiling approach is its clear classification and description of cages and channels in porous structures. As shown in Figure 3 a, the 10-ring helical channel running along

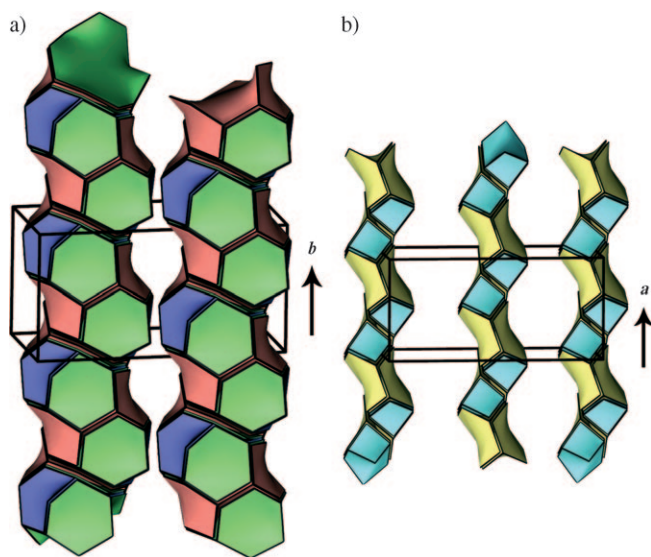


Figure 3. Structural features of CoAPO-CJ40 displayed by tiles. a) Helical channels running along the [010] direction. b) The helical bog columns running along the [100] direction. The face symbols for green, blue, red, cyan, and yellow tiles are [6.10²], [6.10²], [6².10²], [4².6²], and [6³], respectively.

the [010] direction is clearly defined by the linear arrangement of tiles of [6².10²] and [6.10²]. Along the [100] direction, the helical bog column is constructed from the alternation of the tiles of [6³] and [4².6²] (Figure 3 b).

The substitution of Co²⁺ for Al³⁺ in the framework was studied by UV/Vis diffuse reflectance spectroscopy (DRS) and molecular mechanics simulations. The characteristic peaks at 540, 580, and 625 nm in the DRS spectrum (Supporting Information Figure S4) are assigned to tetrahedrally coordinated Co^{II}, which is in agreement with peaks observed in other cobalt aluminophosphates.^[20] In most Co_xAl_(1-x)PO₄ structures, the cobalt atoms are disordered in the framework and difficult to locate at any specified position.^[21] However, in CoAPO-CJ40, the Co atoms exclusively occupy the same Al(1) position with a probability of 50%. This can be easily understood by using a molecular mechanics computation. A structure model with a pure AlPO₄ composition was built by replacing all the Co atoms by Al atoms. The bond angle variance^[22] for each AlO₄/PO₄ tetrahedron was calculated after the geometry of this

structure model was fully optimized. The results show that there is a large bond angle variance on the Al(1) site (4.623, Supporting Information, Table S1), which means that the Al(1)-centered tetrahedron may suffer from high distortion from the ideal tetrahedron. This result implies that the incorporation of Co atoms (or Zn atoms) might be necessary for the framework to relax the high distortion, thus stabilizing the whole structure. It should be noted that pure aluminophosphate AlPO-CJ40 could not be successfully prepared in the absence of Co or Zn ions.

Three other structure models were built by replacing Al(1), Al(2), and Al(3) with Co atoms, respectively. By calculating the framework energy of these three structure models, we can predict that the model with the lowest energy should be the most feasible one. The calculated framework energies of the three optimized models are -9401.35, -9374.83, and -9372.36 kcal mol⁻¹ per unit cell, respectively. The first structure model in which cobalt atoms occupy the Al(1) position should be the most reasonable one. This result agrees well with that from the single-crystal structure analysis.

Several batches of crystals were randomly picked from the bulk product for circular dichroism (CD) measurements. The CD spectra of CoAPO-CJ40 in a KBr pellet all exhibit a positive Cotton effect with strong signals at 500–600 nm (Supporting Information Figure S5). Thus, the resultant crystals are not racemic even though the synthesis did not involve any chiral starting materials. The enantiomeric excess is, in fact, a chiral symmetry breaking effect, which may be explained by an advection-mediated nonlinear autocatalytic process. Cartwright et al. demonstrated that the nucleation of a crystal of one chirality is a symmetry-breaking event on the microscale but the nonlinear autocatalytic dynamics of secondary nucleation amplify this effect to the macroscale to such an extent that the entire chirality may be influenced by the chirality of a single mother crystal.^[23] The chiral symmetry-breaking phenomenon has been observed in a three-dimensional organic-inorganic chiral coordination polymer that exhibits chiral catalytic properties,^[24] a chiral layered coordination polymer Co(pdc)(H₂O)₂·H₂O synthesized by using an achiral ligand pyridine-2,5-dicarboxylic acid (H₂pdc) and a chiral heterobimetallic helical chain complex [(bpca)Fe^{III}(CN)₃Cu(bpca)(H₂O)·H₂O]_n (bpca = bis(2-pyridylcarbonyl) amidate anion) prepared without any chiral reactant.^[25] CD measurements reveal the optical activity of the CoAPO-CJ40.

In summary, novel chiral aluminophosphate-based molecular sieves have been prepared through the introduction of transition-metal ions into the aluminophosphate framework. The metal sites can be unambiguously established by single-crystal structure analysis and molecular mechanics computations. Interestingly, the distribution of the metal ions along the wall of the channels shows a helical arrangement. The CD spectrum of CoAPO-CJ40 exhibits a strong Cotton effect, suggesting that the resultant crystals are not racemic even though the synthesis did not involve any chiral starting materials. More experimental exploration of chiral zeolites is needed. The discovery of a chiral AlPO-type single-site solid catalyst will open up many new applications in the fine-chemical and pharmaceutical industries.

Experimental Section

Synthesis: In a typical synthesis of CoAPO-CJ40 and ZnAPO-CJ40, H_3PO_4 (2.29 mL, 85 wt% in water) was dispersed in a mixture of tetraethylene glycol (8 mL) and H_2O (2 mL) and then $\text{Co}(\text{NO}_3)_2 \cdot 6\text{H}_2\text{O}$ (0.227 g) or $\text{Zn}(\text{NO}_3)_2 \cdot 9\text{H}_2\text{O}$ (0.365 g) and $\text{Al}(\text{O}i\text{Pr})_3$ (0.840 g) were added with stirring. Next, diethylamine (2.92 mL, 99 wt% aqueous solution) was added. A homogeneous gel was formed after stirring for 1 h. The gel was sealed in a teflon-lined stainless steel autoclave and heated at 180 °C for 12 days under static conditions. Blue rectangular single crystals of CoAPO-CJ40 and colorless rectangular single crystals of ZnAPO-CJ40 were separated from the remainder of the product by sonication, washed with distilled water, and then dried in air. Energy-dispersive X-ray detector (EDX) analysis, carried out on JSM-6700F field-emission scanning electron microscope, gave the average molar ratio of Co/Al as 0.2 and (Co + Al)/P equal to 1 for CoAPO-CJ40. Elemental analysis (%; Perkin–Elmer 2400 elemental analyzer) CoAPO-CJ40: calcd: C 5.73, H 1.43, N 1.68; found: C 6.05, H 1.39, N 1.75; ZnAPO-CJ40: calcd: C 5.73, H 0.72, N 1.67; found: C 5.97, H 0.80, N 1.73.

Structure determination: Suitable single crystals with dimensions of $0.23 \times 0.12 \times 0.08 \text{ mm}^3$ for CoAPO-CJ40 and $0.26 \times 0.11 \times 0.10 \text{ mm}^3$ for ZnAPO-CJ40 were selected for single-crystal XRD analysis. Structural analysis was performed on a Siemens SMART CCD diffractometer with graphite-monochromated $\text{MoK}\alpha$ radiation ($\lambda = 0.71073 \text{ \AA}$). The data were collected at a temperature of $T = (20 \pm 2)^\circ\text{C}$. Data processing was accomplished with the SAINT processing program. The structure was solved by direct methods and refined on F^2 by full-matrix least-squares analysis with SHELXTL97. All Co (or Zn), Al, P, and O atoms were easily located. C and N atoms were subsequently located from the difference Fourier map. The protonated diethylamine molecules had an occupancy of 50% according to the elemental analysis and thermogravimetric analysis. The hydrogen atoms in the diethylamine molecules were placed geometrically. All framework atoms were refined anisotropically. Crystal data and details of the structure determination are given in the Supporting Information, Table S2.

Crystal data: CoAPO-CJ40, $M_r = 1675.6$, orthorhombic, space group $P2_12_12_1$ (No. 19), $a = 8.2319(18)$, $b = 9.165(2)$, $c = 17.580(4) \text{ \AA}$, $V = 1326.3(5) \text{ \AA}^3$, $Z = 4$, $\mu = 1.277 \text{ mm}^{-1}$, $\rho_{\text{calcd}} = 2.098 \text{ g cm}^{-3}$, 7870 reflections measured, 2702 unique ($R_{\text{int}} = 0.0657$). The final $wR(F^2)$ (all data) was 0.2026 and $R(F)$ ($I > 2\sigma(I)$) was 0.0753. The flack parameter was 0.18(9). CCDC 690747 contains the supplementary crystallographic data for CoAPO-CJ40.

ZnAPO-CJ40, $M_r = 1688.5$, orthorhombic, space group $P2_12_12_1$ (No. 19), $a = 8.2367(14)$, $b = 9.1664(16)$, $c = 17.550(3) \text{ \AA}$, $V = 1325.1(4) \text{ \AA}^3$, $Z = 4$, $\mu = 1.557 \text{ mm}^{-1}$, $\rho_{\text{calcd}} = 2.116 \text{ g cm}^{-3}$, 8258 reflections measured, 3003 unique ($R_{\text{int}} = 0.0274$). The final $wR(F^2)$ (all data) was 0.1702 and $R(F)$ ($I > 2\sigma(I)$) was 0.0552. The flack parameter was 0.12(3). CCDC 698894 contains the supplementary crystallographic data for ZnAPO-CJ40. These data can be obtained free of charge from The Cambridge Crystallographic Data Centre via www.ccdc.cam.ac.uk/data_request/cif.

Topological analysis: The program 3dt was used for the visualization of all the tiles.^[18] The vertex symbols and coordination sequences (Supporting Information, Table S3), as well the natural tiling were calculated by using the free software TOPOS.^[19]

Molecular mechanics simulations: To describe the interactions among framework atoms, a Burchart force field was introduced, and the Cerius² software package^[26] was used for all computations. Since there were no parameters for a cobalt atom in the Burchart force field, we set all the force constants of the cobalt atom to be the same as those of aluminum atoms. The expected distances of Co–O, O–Co–O, and Co–O–P were set to be 1.96, 3.20, and 3.16 Å, respectively. Coulombic interactions were ignored. The cell param-

eters and all the atoms in the structure models were fully relaxed by using the OFF method in Cerius².

Received: July 23, 2008

Published online: December 3, 2008

Keywords: aluminophosphates · chirality · solvothermal synthesis · transition metals · zeolites

- [1] A. Baiker, *Curr. Opin. Solid State Mater. Sci.* **1998**, 3, 86–93.
- [2] M. M. J. Treacy, J. M. Newsam, *Nature* **1988**, 332, 249–251.
- [3] W. T. A. Harrison, T. E. Gier, G. D. Stucky, R. W. Broach, R. A. Bedard, *Chem. Mater.* **1996**, 8, 145–151.
- [4] T. Cheetham, H. Fejellvag, T. E. Gier, K. O. Kongshaug, K. P. Lillerud, G. D. Stucky, *Stud. Surf. Sci. Catal.* **2001**, 135, 158.
- [5] T. E. Gier, X. H. Bu, P. Y. Feng, G. D. Stucky, *Nature* **1998**, 395, 154–157.
- [6] L. Q. Tang, L. Shi, C. Bonneau, J. L. Sun, H. J. Yue, A. Ojiva, B. L. Lee, M. Kritikos, R. Bell, Z. Bacsik, J. Mink, X. D. Zou, *Nat. Mater.* **2008**, 7, 381–385.
- [7] Y. Li, J. Yu, Z. Wang, J. Zhang, M. Guo, R. Xu, *Chem. Mater.* **2005**, 17, 4399–4405.
- [8] J. H. Yu, R. R. Xu, *J. Mater. Chem.* **2008**, 18, 4021–4030.
- [9] S. T. Wilson, B. M. Lok, C. A. Messian, T. R. Cannan, E. M. Flanigen, *J. Am. Chem. Soc.* **1982**, 104, 1146–1147.
- [10] a) J. H. Yu, R. R. Xu, *Chem. Soc. Rev.* **2006**, 35, 593–604; b) J. H. Yu, R. R. Xu, *Acc. Chem. Res.* **2003**, 36, 481–490; c) Y. Li, J. H. Yu, R. R. Xu, Database of AlPO Structures, <http://crystals.ethz.ch:9006/alpo/>.
- [11] J. M. Thomas, R. Raja, *Proc. Natl. Acad. Sci. USA* **2005**, 102, 13732–13736.
- [12] J. M. Thomas, R. Raja, G. Sankar, R. G. Bell, *Acc. Chem. Res.* **2001**, 34, 191–200.
- [13] J. M. Thomas, R. Raja, *Microporous Mesoporous Mater.* **2007**, 105, 5–9.
- [14] J. M. Thomas, R. Raja, *Acc. Chem. Res.* **2008**, 41, 708–720.
- [15] a) L. Gómez-Hortigüela, F. Corà, C. R. A. Catlow, J. Pérez-Pariente, *Phys. Chem. Chem. Phys.* **2006**, 8, 486–493; b) L. Gómez-Hortigüela, C. Márquez-Álvarez, E. Sastre, F. Corà, J. Pérez-Pariente, *Catal. Today* **2006**, 114, 174–182.
- [16] P. Y. Feng, X. H. Bu, G. D. Stucky, *Nature* **1997**, 388, 735–740.
- [17] C. Baerlocher, L. B. McCusker, D. H. Olson, *Atlas of Zeolite Framework Types*, 6th rev. ed., Elsevier, Netherlands, **2007**; IZA Structure Commission website: <http://www.iza-structure.org/databases/>.
- [18] O. Delgado-Friedrichs, M. O’Keeffe, *Acta Crystallogr. Sect. A* **2003**, 59, 351–360.
- [19] V. A. Blatov, O. Delgado-Friedrichs, M. O’Keeffe, D. M. Proserpio, *Acta Crystallogr. Sect. A* **2007**, 63, 418–425.
- [20] A. A. Verberckmoes, M. G. Uytterhoeven, R. A. Schoonheydt, *Zeolites* **1997**, 19, 180–189.
- [21] P. A. Wright, M. J. Maple, A. M. Z. Slawin, V. Patinec, R. A. Aitken, S. Welsh, P. A. Cox, *J. Chem. Soc. Dalton Trans.* **2000**, 1243–1248.
- [22] K. Robinson, G. V. Gibbs, P. H. Ribbe, *Science* **1971**, 172, 567–570.
- [23] J. H. E. Cartwright, J. M. García-Ruiz, O. Piro, C. I. Sainz-Díaz, I. Tuval, *Phys. Rev. Lett.* **2004**, 93, 035502–1–035502–4.
- [24] A. Monge, N. Snejko, E. Gutiérrez-Puebla, M. Medina, C. Cascales, C. Ruiz-Valero, M. Iglesias, B. Gómez-Lor, *Chem. Commun.* **2005**, 1291–1293.
- [25] a) G. Tian, G. Zhu, X. Yang, Q. Fang, M. Xue, J. Sun, Y. Wei, S. Qiu, *Chem. Commun.* **2005**, 1396–1398; b) H. Wen, C. Wang, J. Zuo, Y. Song, X. Zeng, X. You, *Inorg. Chem.* **2006**, 45, 582–590.
- [26] Cerius² 4.6; © Accelrys Inc.; **2001**.